A computational environment for hypernuclear structure calculations

Gustav R. Jansen <gustavj@math.uio.no>

May 8, 2008

Contents

List of Figures

List of Tables

1 Introduction

A proper introduction to the thesis goes here.

My goal in this thesis is to present an efficient computational for hypernuclear structure calculations. By efficient I mean that different models can easily be plugged into the existing framework, so that the user can concentrate more on actual physics than programming logic. To make this possible, it's necessary to combine a powerful scripting language with the computational efficiency of a lower-level compiled language.

It should also be possible to extend the calculations to include more baryons and many-body forces as these become feasible. It should be easy to look at specific data, which includes some visualisation (graph/animation). The calculation should be numerically precise, so that the data can be used quatitativly as well as qualitativly. There shoudn't be any constraints on the size of the systems calculated. It should be parallellized and variations on different input parameters should be easy to accomplish.

Aftermarket tools to process data should be easy to include.

*** Some of this should evidently go into a chapter on the design/reasoning of writing the software.

From heyde WHen starting the study of the nuclear many-body system, it's a good idea to ask how one best describes such a system. Should the nucleus be considered as a system where single-partielc degrees of freedom dominate and determine the observed nuclear structure phenomena. Can the nucleus be described as a charged liquid drop rotating and vibrating. Is it more cvorrect to speak of nucleons and nucleon resonances in a meson field, or should we go down to the deepest levels of quarks interacting with gluon fields to descibe what we observe in the nucleus.

The way in which the nucleus can be observed and described is determined by the energy scale by which we observe. As a collective, the nucleus displays quite alot of ordered motion in spite of the strong nature of the interaction.

The nuclear shell model proves that nucleon correlations of a limited number of protons and neutrons outside a closed shell configuration descirbe a large variety of nuclear excited state properties.

In this thesis I present a tool for studying hypernuclear stucture. The intended goal was to create a framework that would allow structure calculations using the shell-model approach, or a coupled cluster approach, starting from a realistic two-body interaction. It was ofcourse to be possible to extract data at every step of the process and each step should be completely autonomous, so that it could be exchanged easily with similar procedures. The effects of this exchange on the data, could be studied immediately.

Even though most of the groundwork was laid out for the nuclear case, this goal prove to be overly optimistic. I had to stop at calculating a selfconsistent single-

particle basis for a selected set of closed core nuclei, with a Λ in a low orbital around this. But allready at this stage, the results using different interaction models, proved to be very different and a converged result for could not be obtained.

As interaction models get constrained by more scattering data from new experiment, these models can easily be included in this framework and new in a matter of hours I can produce results with the new model.

It might be more reasonable to use a g-matrix approach for the two-body renormalized interaction, but this will introduce an energy dependent effective interaction that has to be taken care of in the code.

If I'm allowed to continue with this work, that would be one of the first extension applied.

2 Background

3 Software

4 The many-body problem

5 Theory

6 Applications

7 Results

7.1 The bare and renormalized interaction in specific channels

7.1.1 Proton proton case

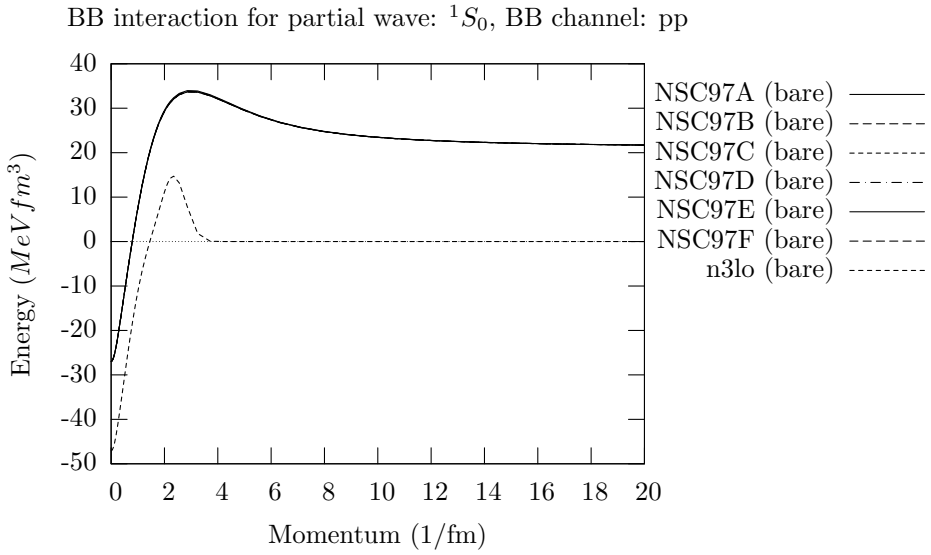

Figure 7.1: Bare interaction

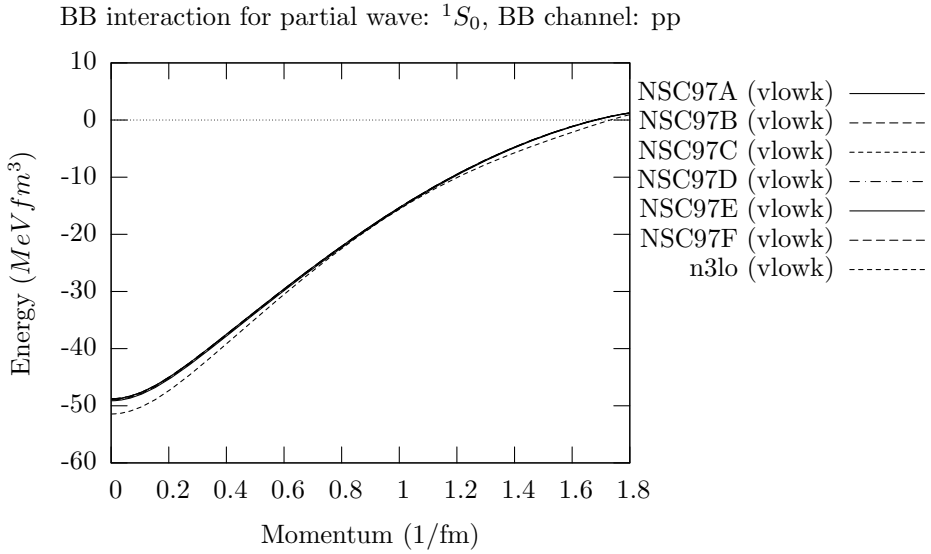

Figure 7.2: cutoff = 1.8

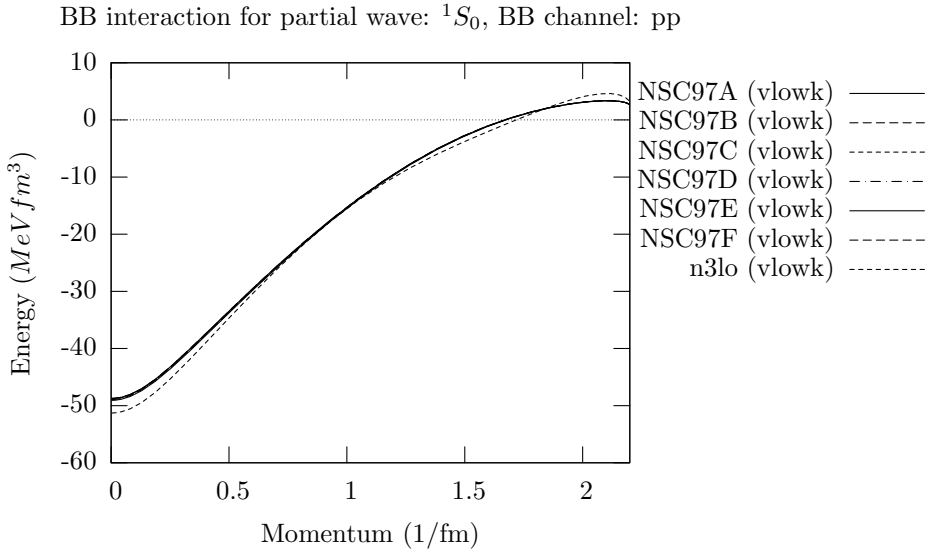

Figure 7.3: cutoff = 2.2

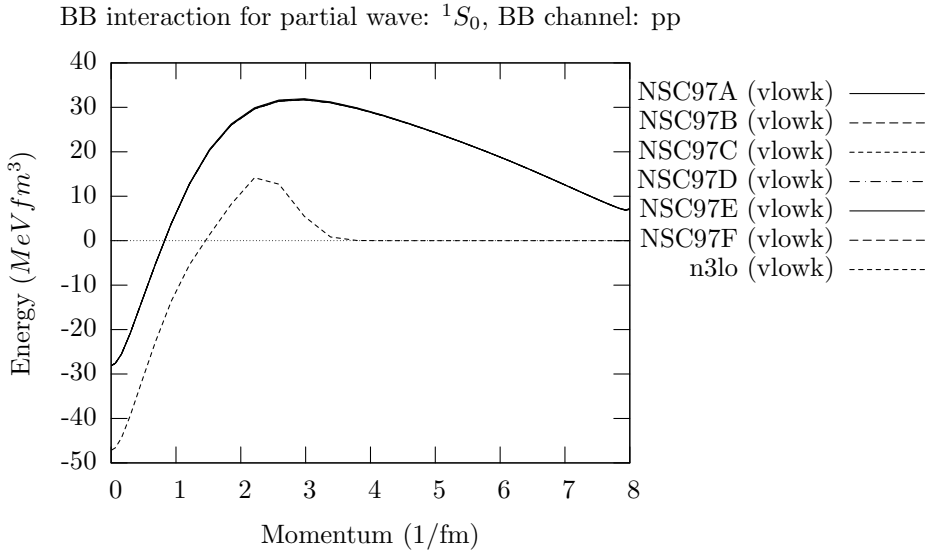

Figure 7.4: cutoff = 8.0

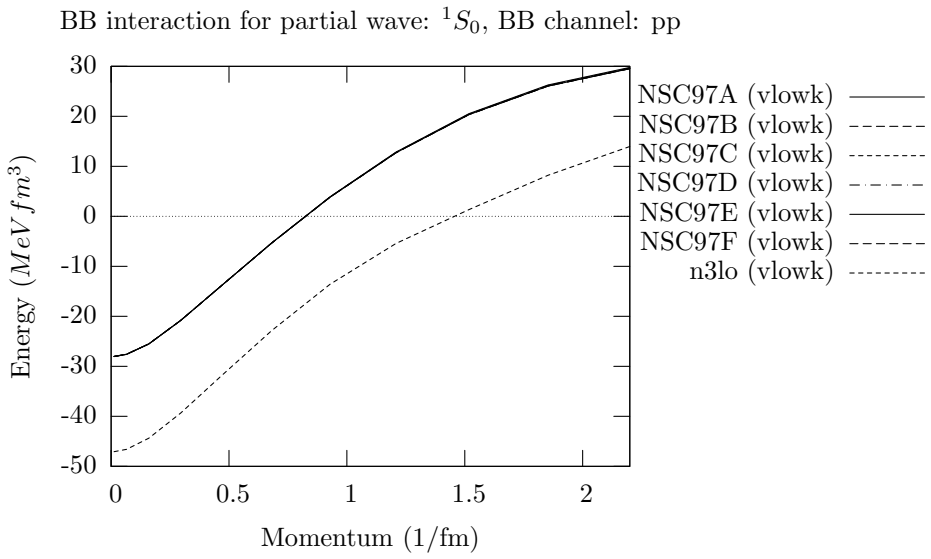

Figure 7.5: cutoff = 8.0

7.1.2 Proton neutron case

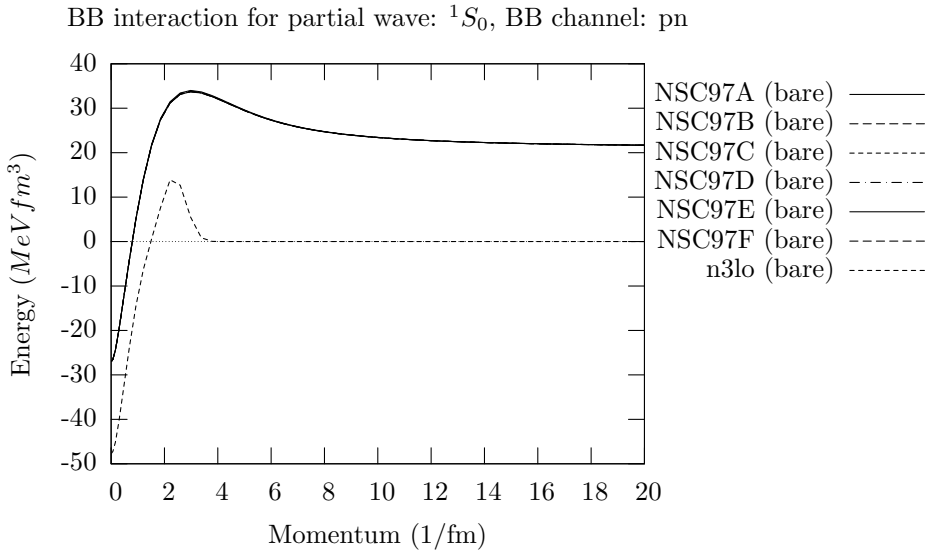

Figure 7.6: Bare interaction

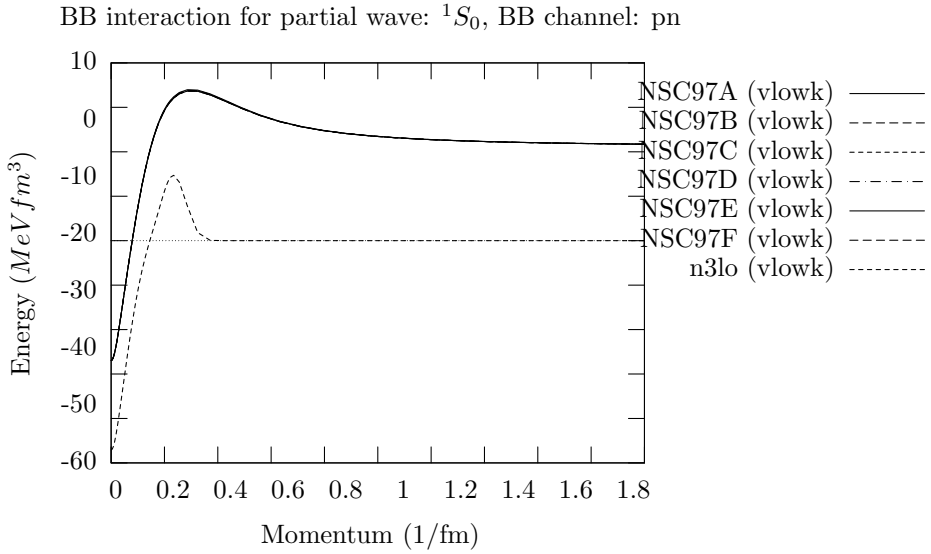

Figure 7.7: cutoff = 1.8

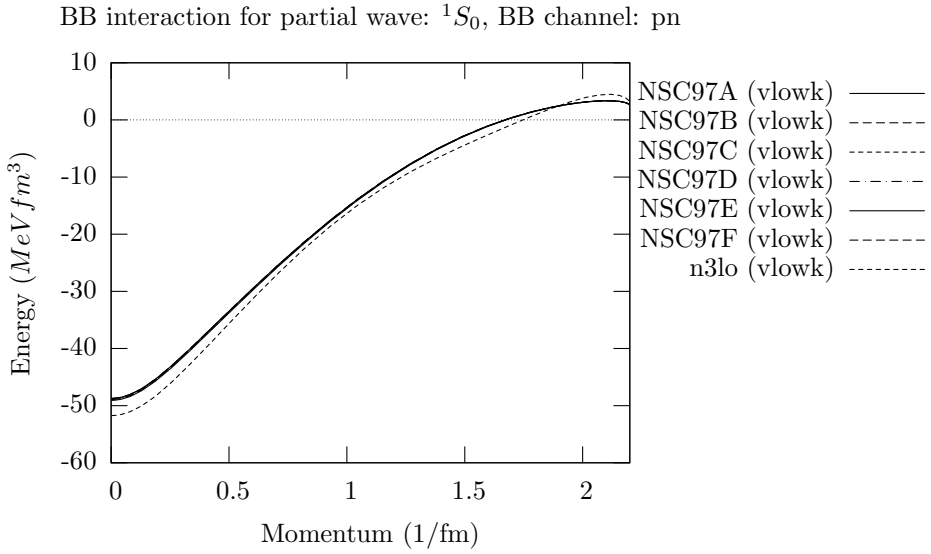

Figure 7.8: cutoff = 2.2

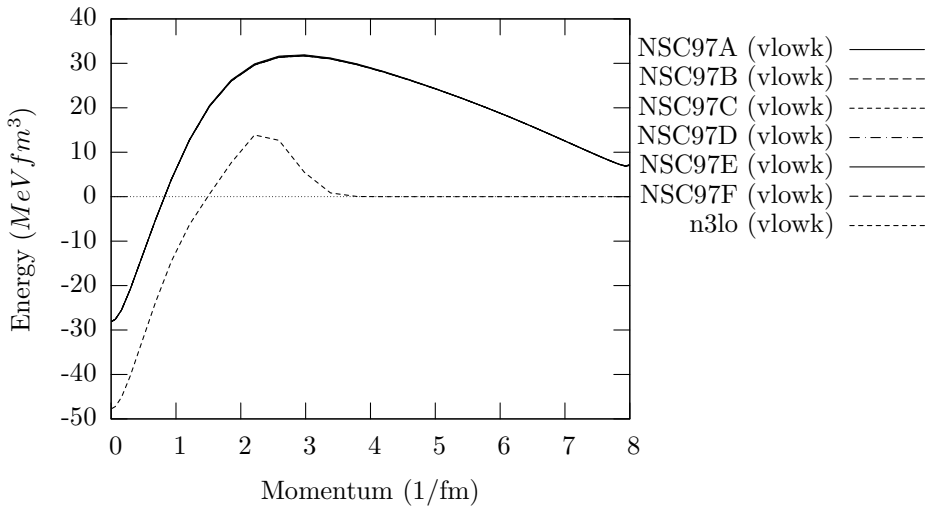

Figure 7.9: cutoff = 8.0

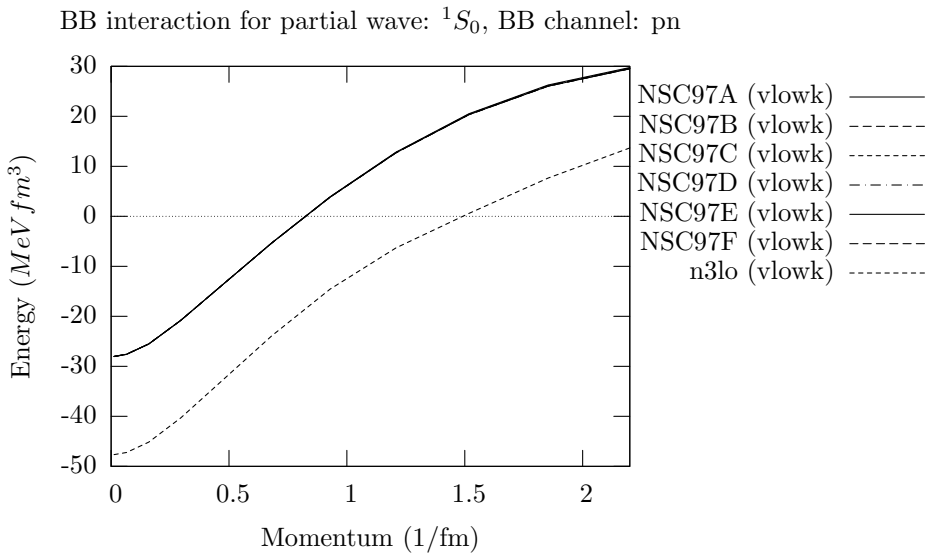

Figure 7.10: cutoff = 8.0

7.1.3 Neutron neutron case

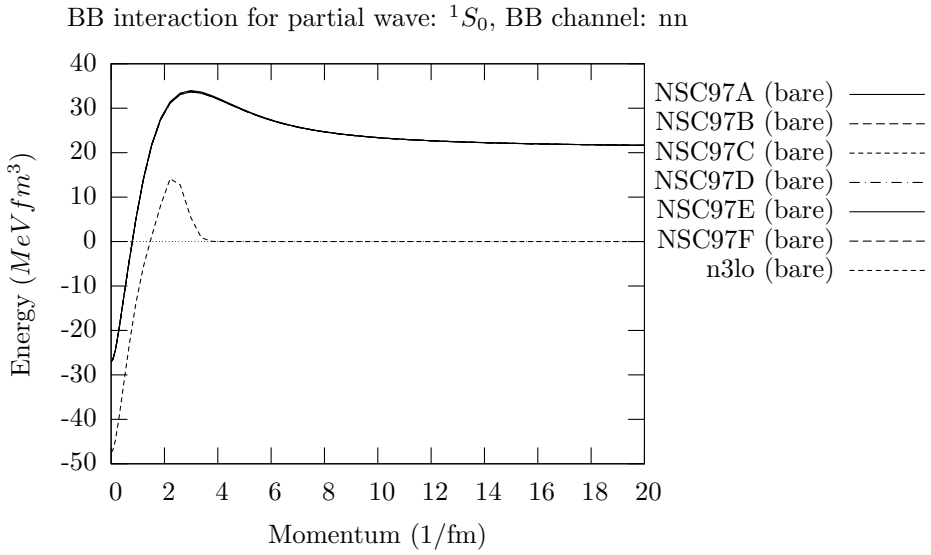

Figure 7.11: Bare interaction

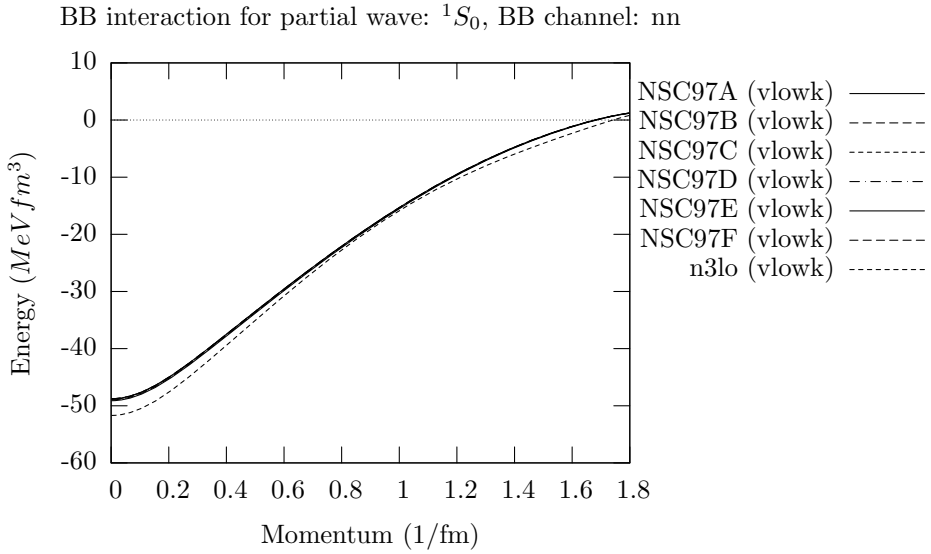

Figure 7.12: cutoff = 1.8

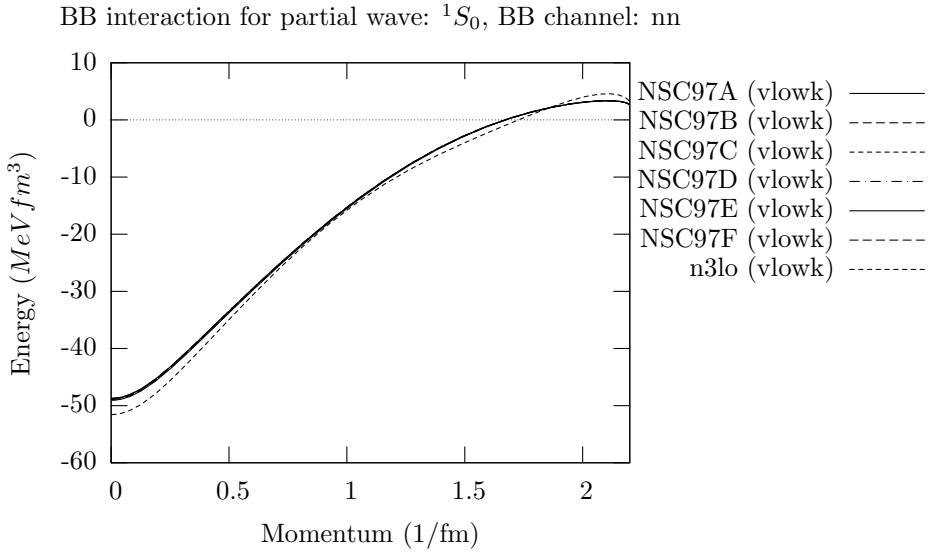

Figure 7.13: cutoff = 2.2

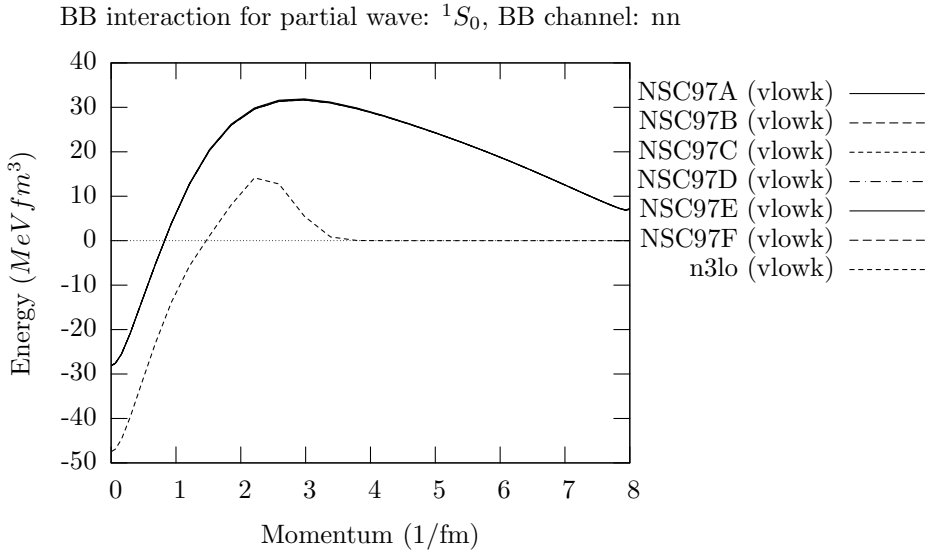

Figure 7.14: cutoff = 8.0

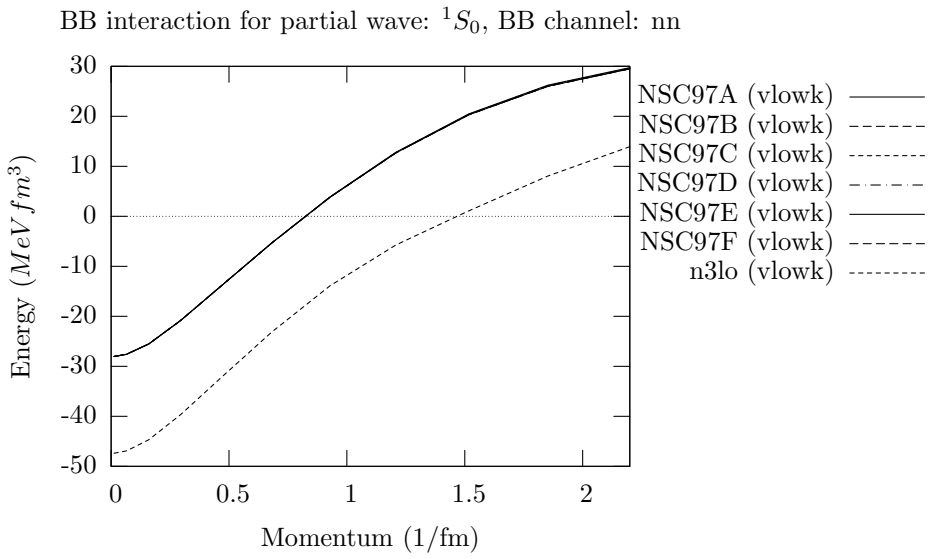

Figure 7.15: cutoff = 8.0

7.2 Testcases

7.2.1 Experiment 1 - Choosing the number of meshpoints

The vlowk renormalization procedure, as well as the transformation from a basis in telative momentum wavefunctions, to relative harmonic oscillator wavefunctions, both require an integration over momentum k with $k \in [0, \infty]$. Numerically, this would normall be accomplished by selecting the meshpoints by a tangent mapping in the domain. When doing vlowk however, we will be projecting the problem to a smaller space defined by $k \in [0, \lambda]$, where λ is in the area of $2fm^{-1}$. We therefore need a certain amount of meshpoints inside the modelspace. A tangent mapping will generate too few points in the modelspace, with too many in the complement space, so we will have to rething this approach.

By using the fact that the interaction models we are using, have a limited domain of validity, we can introduce a cutoff k_max in the complement space and integrate over the domain $k \in [0, k\_max]$ instead of $k \in [0, \infty$. We would have to select k_max large enough that the results converge an is independent of the choice of k_max. We can the choose a definite set of integration points inside the modelspace, and another set of integration points in the complement space. The number of meshpoints will ofcourse also be selected so that the results are independent of the number of meshpoints.

Figure 7.16 and 7.17 shows the dependence of the lowest energy eigenvalue on the number of meshpoints in the tensor coupled channel ${}^3s - d_1$, for the pn and Λp cases respectivly. Note that the number of meshpoints indicated is for an uncoupled channel, so that the dimension of the problem in a tensor coupled channel is twice the number of meshpoints. The latter channel is also a baryon coupled channel with 3 subchannels, so the dimension of the hamiltonian is 6 times the number of meshpointsfor this problem.

Both these figures shows relativly rapid convergence with the number of meshpoints and we choose 60 meshpoints as a reasonable number for the rest of our calculations. This gives 30 meshpoints in the modelspace and 30 in the complement space.

This choice of meshpoints also gives unity to 6 significant figures when normalizing the overlap between the relative momentum wavefunction and the harmonic oscillator wavefunction. This is more than acceptable.

Using 60 meshpoints seems to give converged eigenvalues for all channels and interaction models. In addition this gives unity to 5 significant figures when setting up the square of the total radial ho wavefunction.

Choosing to run with 60 meshpoints, where 30 are in the modelspace and 30 in the complement space.

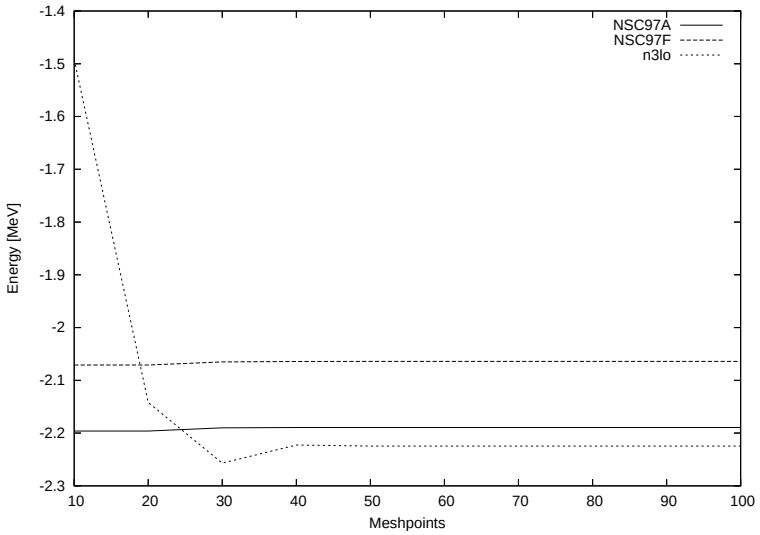

Figure 7.16: Energy eigenvalues for pn in ${}^3s_1$ as a function of the number of meshpoints,

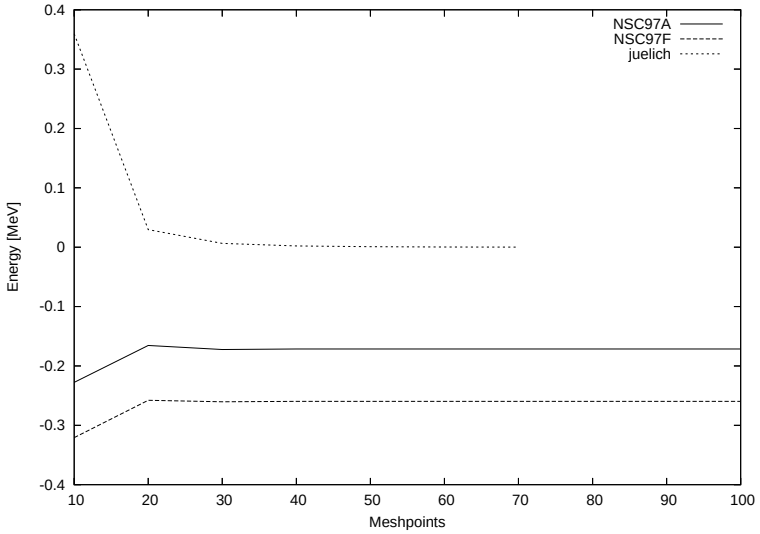

Figure 7.17: Energy eigenvalues for Λp in ${}^3s_1$ as a function of the number of meshpoints. Note that the code for the juelich interaction doesn't support more than 70 meshpoints.

7.2.2 Experiment 2 - Choosing the cutoff in complement space

Energy eigenvalues as a function of the number of kmax

Figure 7.18 and 7.19 shows the eigenvalues of the ${}^3s-d_1$ tensor coupled channel in the pn case and the baryon coupled Λp case as a function of the momentum cutoff of the complement space. It seems clear that a reasonable cutoff can be chosen to be $k\_max = 20fm^{-1}$ to be sure the results is not dependent on the choice of cutoff.

juelich and nijmegen differ, especially in the high k elements.

Defining a Q spacxe cutoff of $20fm^{-1}$ gives reasonable convergence of the emergy eigenvalues.

7.2.3 Eexperiment 3 - Which NSC97 models should be chosen

1. Show no differnce in uncoupled channels. 1s0 s+p and 1 more plot and wigenvalues

2. Show differences in coupled channels. Tensor and baryon couplings. 3. Show difference after vlowk. Plot both bare and renormalized. 3 models in a single plot, makes 6 dataset pr. plot. 4. Show the difference in the matrix elements that add up to selfenergy in 0th order HF.

5. Show the difference in the lambda self-energies.

Run for l=7, n = 3 0/3 for hyperons. $\hbar\omega = 10.0$ cutoff is 2.5 with 30 points.

7.2.4 Experiment 4

Reproduction of the eiganvalues with the largest contribution from the modelspace.

In the proton-neutron case. The bound state has some contribution from the Q space, but most from the modelspace. All exclude eigenvalues have eigenvectors with small (≤ 0.01) projections in the modelspace.

In the Λ-proton case. The bound state has an 80% contribution from the Q-space, but still a considerable contribution from the modelspace. 2 eigenvalues with considerable contributions from the modelspace are excluded. Increasing the size of the modelspace would include this eigenvalue. Tested with $\lambda = 4$.

7.2.5 The deuteron

The deuteron is the two-body system consisting of a proton and a neutron. This is the only experimentally observed bound two particle state and presents an ideal testcase for the interaction models. The deuteron is a result of a bound

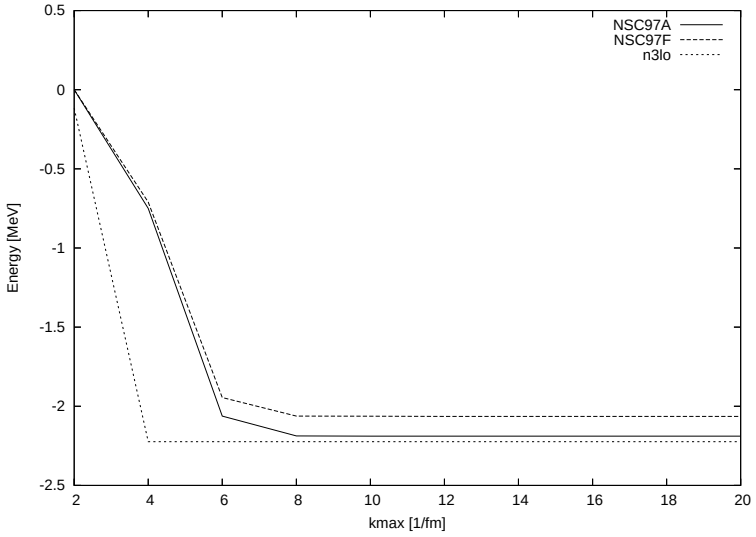

Figure 7.18: Energy eigenvalues for pn in ${}^3s_1$ as a function of the maximum momenta.

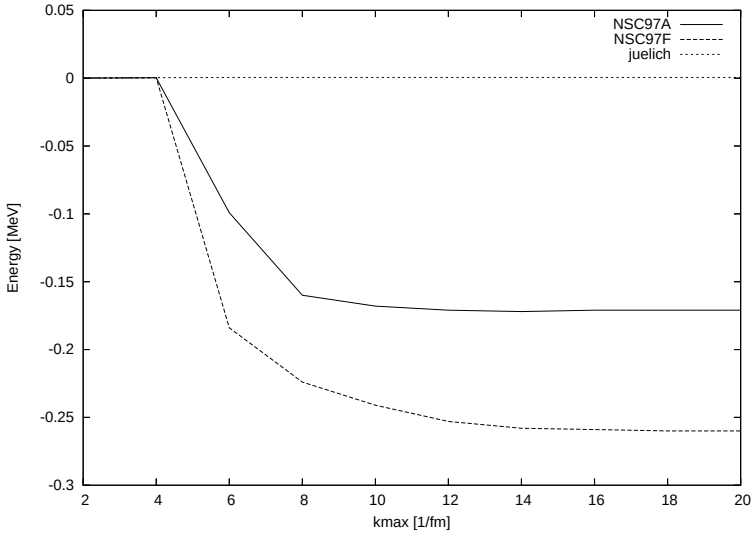

Figure 7.19: Energy eigenvalues for Λp in ${}^3s_1$ as a function of the maximum momenta.

Eigenvalue	Reproduced eigenvalue	Component in modelspace
3.416601064070259e-02	3.41660106e-02	0.999999999992494
0.913903152314748	0.913903152	0.999999753686008
5.18630750445118	5.18630750	0.999974849789549
4.516991861981452e-02	4.51699186e-02	0.999958631124156
16.4629477952448	16.4629478	0.999758927293190
37.7695969033269	37.7695969	0.999108809044036
69.3632452801311	69.3632453	0.997653026322953
1.67204257152620	1.67204257	0.997582563473404
195.194304801923	195.194305	0.994676613576324
107.812877403660	107.812877	0.994535352050002
9.76155442131280	9.76155442	0.993109180996088
28.4094550039271	28.4094550	0.989205524579391
173.255007035140	173.255007	0.988438865803158
146.799723753018	146.799724	0.988372255392941
58.6794630832711	58.6794631	0.985687987040545
138.349146335824	138.349146	0.984494304532942
-2.19710759140494	-2.19710759	0.984457926217859
97.4994811462420	97.4994811	0.983668484782110
178.935732589212	178.935733	0.979172364286131
197.909623323750	197.909623	0.975195198852643
271.883233439369		7.102835286156098e-002
596.099991172277		4.854211803254944e-002
1492.54639803869		1.805410080982251e-002
247.718642318589		1.047373856972548e-002
3474.87162141087		6.363343100272794e-003
559.658434811425		5.088947011829431e-003
1564.65534547262		3.818912188671142e-003
6614.59502627771		1.185214809276037e-003
10401.2967031056		1.815889093970478e-004
7121.68371265130		7.510327242621864e-005
3735.20336991250		5.425637132750700e-005
13783.0881807160		3.469573388278385e-005
10970.2187921564		2.180550537412961e-005
20164.6648712114		1.052273828274194e-005
15931.5067321025		7.901703897141228e-006
14221.9419099527		5.285175464116271e-006
16166.6721877254		1.605607634895445e-006
21063.4672720451		1.326855932755532e-006
34727.7534440951		5.451528507677166e-007
35663.7515013417		1.675389847408723e-008

Table 7.1: Eigenvalues for deuterium ${}^3s - d_1$

Eigenvalue	Reproduced eigenvalue	Component in modelspace
3.268651738859335e-02	3.26865174e-02	0.999999698416531
2.923637269837017e-02	2.92363727e-02	0.999998156522386
2.367334246202904e-02	2.36733425	0.999985258477301
0.942226667923387	0.942226668	0.999981379442691
0.731771165862715	0.731771166	0.999909601583194
5.53410662992936	5.53410663	0.999815158762751
0.534697917194415	0.534697917	0.999579427757253
4.11705074370058	4.11705074	0.999451113944257
17.4391960392881	17.4391960	0.999113356242823
3.23935374704335	3.23935375	0.998525218000787
13.4268335487878	13.4268335	0.998459859370169
11.6039468196882	11.6039468	0.997160991467505
39.2031242675101	39.2031243	0.997097568295071
31.8611897324750	31.8611897	0.996914621528358
29.2031930562889	29.2031931	0.995349116099256
60.3037585720680	60.3037586	0.994658865274222
57.1011197117443	57.1011197	0.992685677360692
70.3989437522830	70.3989438	0.992253881071362
95.8942702495549	95.8942702	0.991344972135024
92.3621046354053	92.3621046	0.988635948332279
132.571143429431	132.571143	0.986442851286620
128.708303112619	128.708303	0.982663006480691
106.761328765209	106.761329	0.981597878473652
163.011430480446	163.011430	0.978891471256576
176.445063550510	176.445064	0.975582557725821
158.741971793430	158.741972	0.975515622588271
181.135332038870	181.135332	0.963863220556515
141.514315796328	141.514316	0.960809840060427
167.959290986953	167.959291	0.938036674767626
185.443052743800	185.443053	0.720107156802245
318.876718966845		0.191577989416503
-755.418950911826		0.187529153367256
780.831303883140		5.035996804574255e-002
616.229915880355		3.116679806819013e-002
244.825262568516		3.010173830215701e-002
247.094266213475		2.649039023687568e-002
1725.56053398083		2.301748522367679e-002
585.895549337287		1.912477185283220e-002
1587.30022947448		1.356064536574410e-002
3893.91398477343		7.959289370681364e-003
3589.69723185945		6.100199796512800e-003
1849.61252135105		3.935172656286296e-003
6985.70016626551		1.664626177825600e-003
⋮		⋮

Table 7.2: Eigenvalues for $\Lambda - p\ ^1s_0$

state in the ${}^3s - d_1$ tensor coupled channel and the energy of this bound state is -2.224 Our NN interaction models should be able to reprduce this bound state in the specified channel. Figure 7.20 shows the result of diagonalizing the tensor coupled ${}^3s - d_1$ channel for interaction models NSC97A, NSC97F and n3lo. Maybe the most striking observation, is that the NSC97 models does not reproduce the energy of the deuteron bound state, even though they are close. This result is converged and does not improve with increasing the number of meshpoints or the Q-space cutoff. We will therefore not use the NSC97 models for NN interaction, only n3lo. The NSC97 A and F models will be used for the YN and YY interaction.

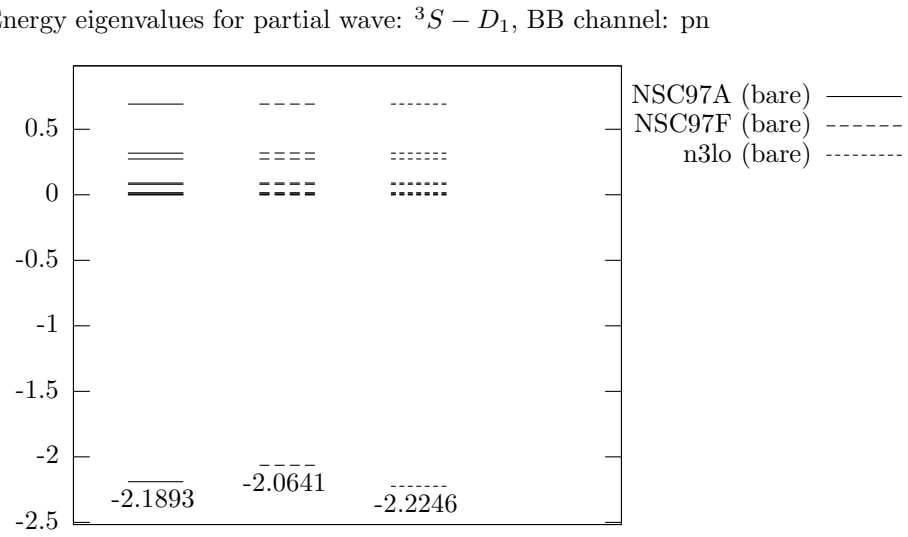

Figure 7.20: Energy eigenvalues for the deuteron in the tensor coupled ${}^3S - D_1$ for NSC97A, NSC97F and n3lo.

The figures 7.21, 7.22 and 7.23 shows the diagonal matrix elements of the ${}^3S_1$, ${}^3D_1$ and the tensor coupling ${}^3S - D_1$ respecticly. The first point to notice, is that the Idaho n3lo model is a chiral interaction model and is only valid for low momentum. Above $k \approx 4fm^{-1}$, all elements are zero. The NSC97 models are however soft-core models and are available for high k also. Allthough the two models are fitted to the same scattering data, their treatment of the different transitions are very different. The Idaho n3lo model has more attraction in the ${}^3S_1$ and ${}^3D_1$ diagonal elements, with more repulsion in the off diagonal ${}^3S - D_1$ elements.

Allthough these interaction models are completely different also in the uncoupled channels, since they are fitted to the same data, the energy eigenvalues in these channels are still the same. In all other tensor coupled channel, the results are also the same, but the ${}^3S - D_1$ channel, which is the most important for the deuteron is not reproduces accurate enough in the NSC97 models.

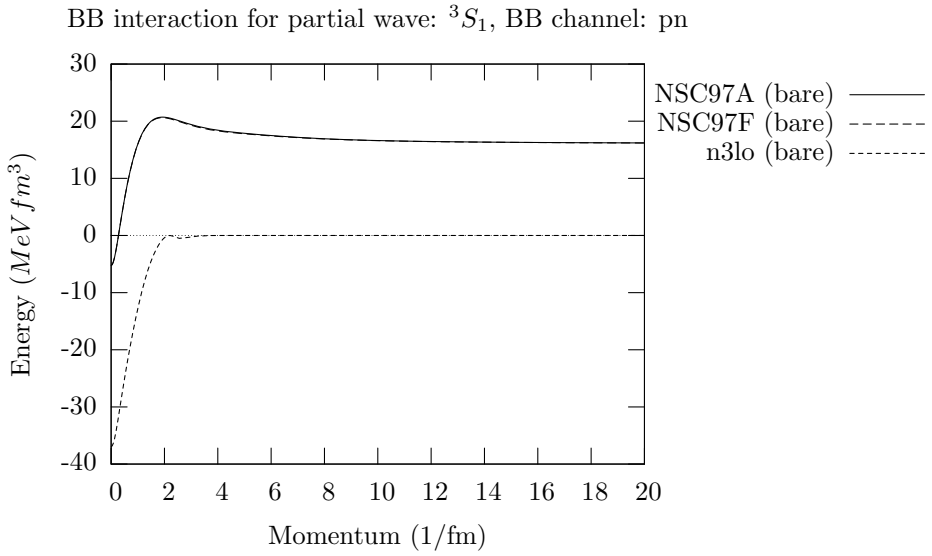

Figure 7.21: Diagonal elements of the $^3S_1$ interaction for the deuteron.

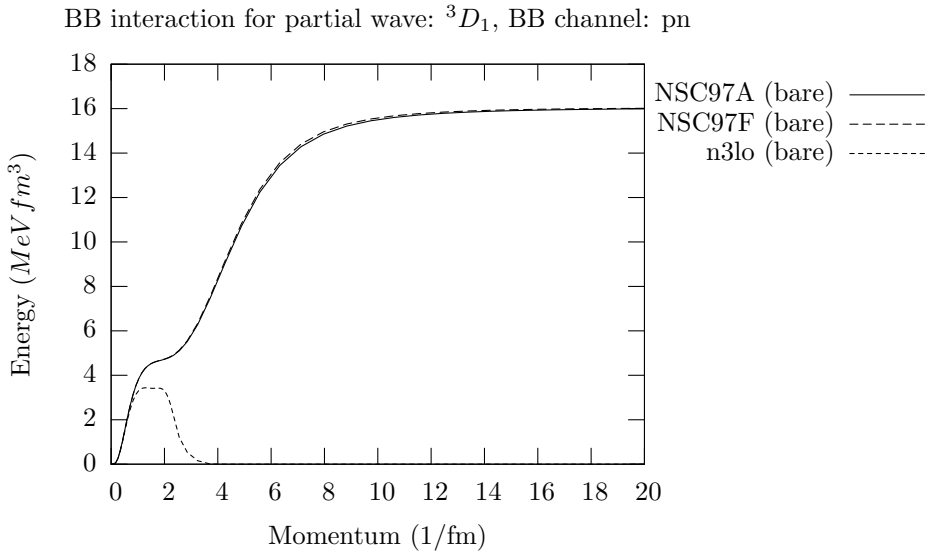

Figure 7.22: Diagonal elements of the $^3D_1$ interaction for the deuteron.

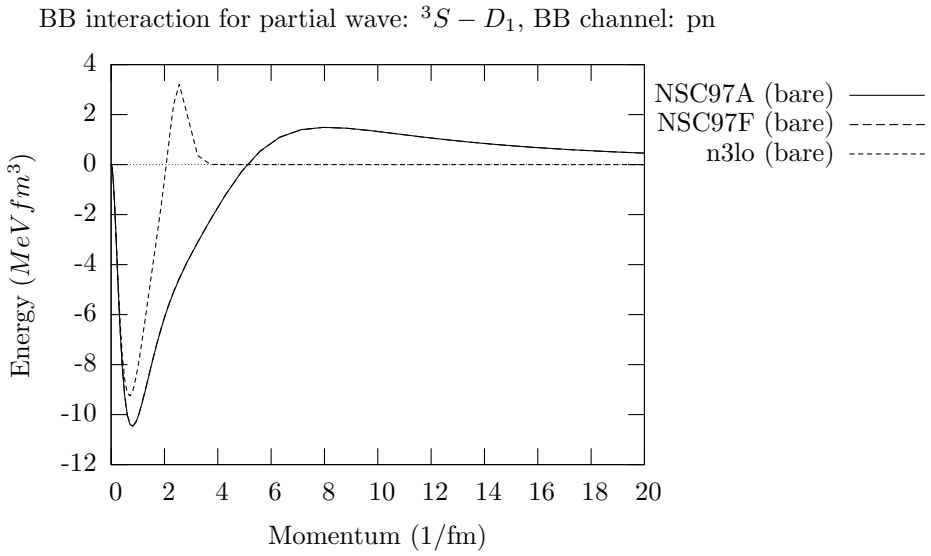

Figure 7.23: Diagonal elements of the $^3S - D_1$ interaction for the deuteron.

7.3 Hyperon nucleon channels

7.3.1 q = -1

7.3.2 q = 0

7.3.3 q = 1

7.3.4 q = 2

7.4 Effective interactions and sp energies

7.4.1 How big is the effect of baryon coupling?

Run with and without baryon couplings: Show: eigenvalues matrix elements sp energies O16 only

7.4.2 Convergence of $\hbar\omega$ with the number of shells included.

Run 3/1, 5/2, 7/3 and 9/4 for $\hbar\omega = 5, 10, 15, 20, 25$

Plot sp energies as function of $\hbar\omega$ for all 4 datasets in the same plot.

Do for 3 interaction models. Plot for O, Ca and Zr

7.4.3 Dependence of sp energies on cutoff and $\hbar\omega$

sp energies for all variations for all cores. Maybe also for different partialces.

7.5 ^{16}O

7.6 ^{40}Ca

7.7 ^{91}Zr

$\hbar\omega$	k_cutoff	NSC97A	NSC97F	Juelich
5.0	2.0	-.142130E+02	-.146005E+02	-.236463E+01
5.0	2.5	-.100220E+02	-.105153E+02	-.145238E+01
5.0	3.0	-.580315E+01	-.621929E+01	-.585954E+00
10.0	2.0	-.283548E+02	-.264695E+02	-.508280E+01
10.0	2.5	-.176048E+02	-.166459E+02	-.228835E+01
10.0	3.0	-.765527E+01	-.718411E+01	0.269105E+00
15.0	2.0	-.343005E+02	-.301819E+02	-.522945E+01
15.0	2.5	-.182380E+02	-.159281E+02	-.570465E+00
15.0	3.0	-.573403E+01	-.417381E+01	0.280576E+01
20.0	2.0	-.353245E+02	-.294330E+02	-.371252E+01
20.0	2.5	-.164269E+02	-.126355E+02	0.202292E+01
20.0	3.0	-.284581E+01	0.692835E-01	0.572580E+01
25.0	2.0	-.341553E+02	-.265827E+02	-.149092E+01
25.0	2.5	-.135103E+02	-.812080E+01	0.498695E+01
25.0	3.0	0.490273E+00	0.497532E+01	0.879451E+01

Table 7.3: Single particle energies for Λ in the $0s_{1/2}$ orbital outside a core of ^{16}O

$\hbar\omega$	k_cutoff	NSC97A	NSC97F	Juelich
5.0	2.0	-.249132E+02	-.248547E+02	-.591739E+01
5.0	2.5	-.180783E+02	-.181185E+02	-.437293E+01
5.0	3.0	-.113244E+02	-.112121E+02	-.299530E+01
10.0	2.0	-.509021E+02	-.440472E+02	-.132682E+02
10.0	2.5	-.330701E+02	-.277015E+02	-.837402E+01
10.0	3.0	-.164776E+02	-.127420E+02	-.399717E+01
15.0	2.0	-.642515E+02	-.490546E+02	-.173640E+02
15.0	2.5	-.354149E+02	-.256347E+02	-.771858E+01
15.0	3.0	-.142093E+02	-.821421E+01	-.141636E+01
20.0	2.0	-.671886E+02	-.470663E+02	-.175821E+02
20.0	2.5	-.332148E+02	-.206469E+02	-.515134E+01
20.0	3.0	-.113397E+02	-.284464E+01	0.135490E+01
25.0	2.0	-.660513E+02	-.428834E+02	-.159834E+02
25.0	2.5	-.303610E+02	-.150148E+02	-.240329E+01
25.0	3.0	-.844995E+01	0.326465E+01	0.392458E+01

Table 7.4: Single particle energies for Λ in the $0s_{1/2}$ orbital outside a core of ^{40}Ca

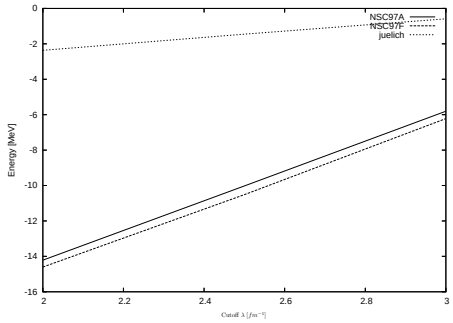

(a) $\hbar\omega = 5$

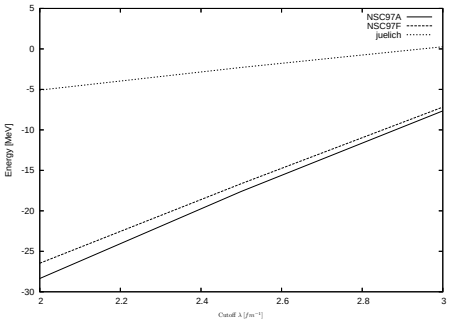

(b) $\hbar\omega = 10$

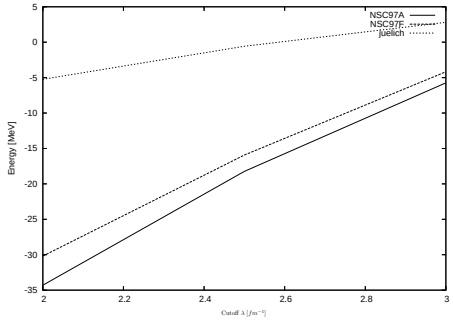

(c) $\hbar\omega = 15$

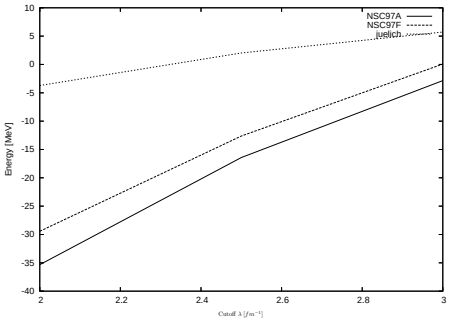

(d) $\hbar\omega = 20$

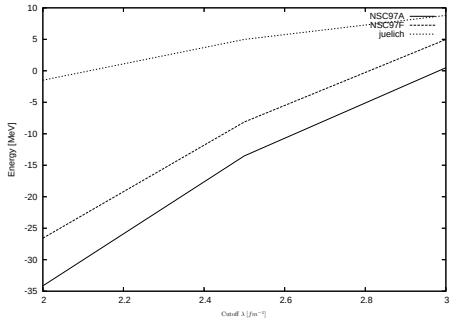

(e) $\hbar\omega = 25$

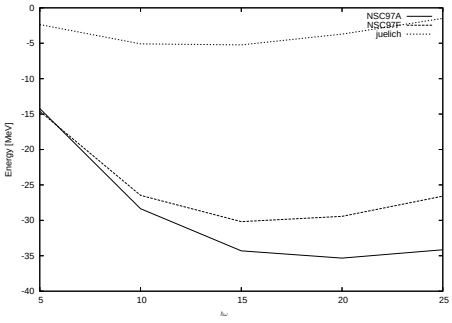

(f) $k\_cutoff = 2.0$

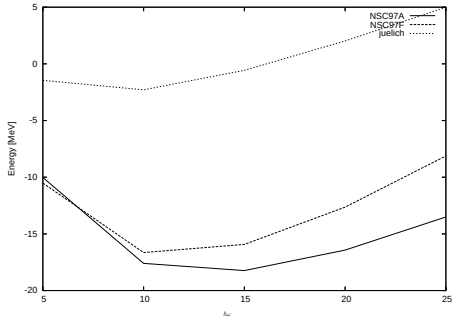

(g) $k\_cutoff = 2.5$

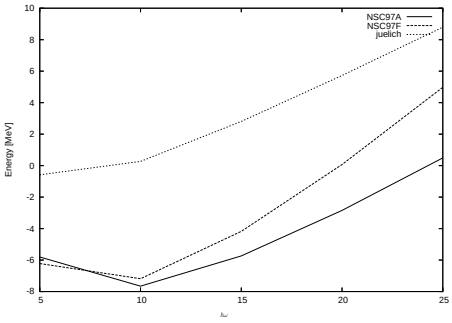

(h) $k\_cutoff = 3.0$

Figure 7.24: Single particle energies in $0s_{1/2}$ for $^{17}_{\Lambda}O$

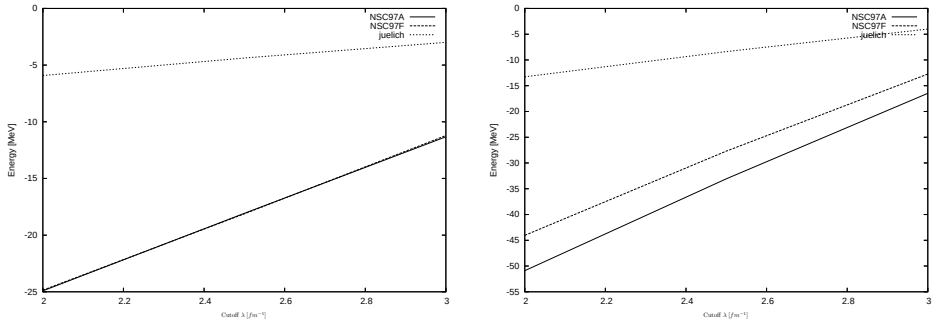

(a) $\hbar\omega = 5$

(b) $\hbar\omega = 10$

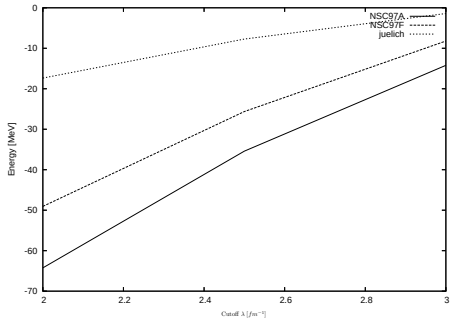

(c) $\hbar\omega = 15$

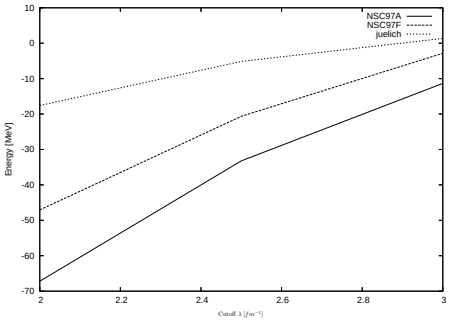

(d) $\hbar\omega = 20$

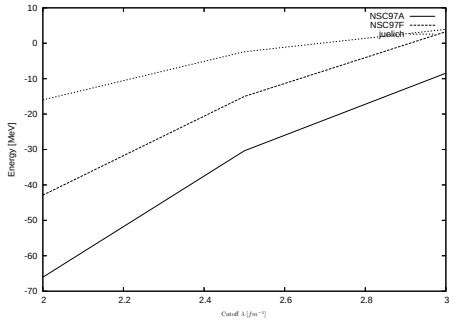

(e) $\hbar\omega = 25$

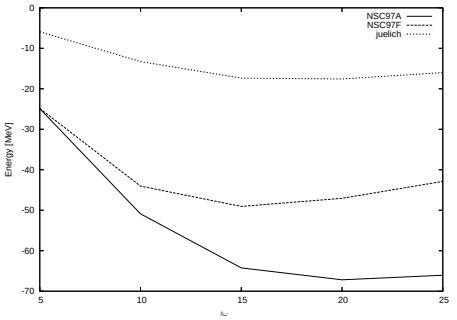

(f) $k\_cutoff = 2.0$

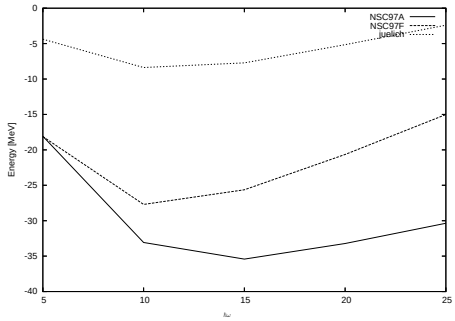

(g) $k\_cutoff = 2.5$

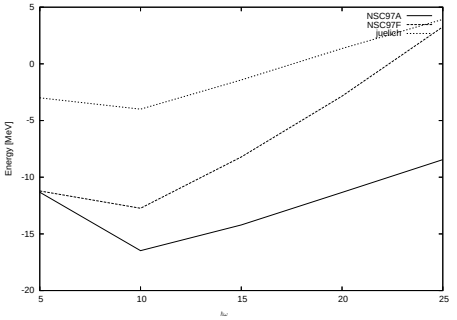

(h) $k\_cutoff = 3.0$

Figure 7.25: Single particle energies in $0s_{1/2}$ for ${}^{41}_{\Lambda}Ca$

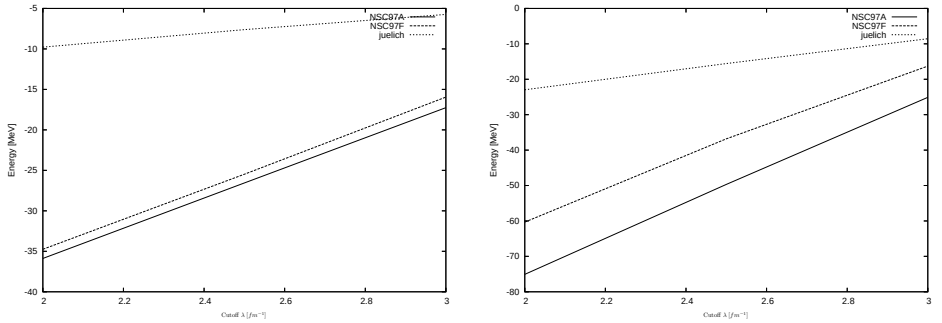

(a) $\hbar\omega = 5$ (b) $\hbar\omega = 10$

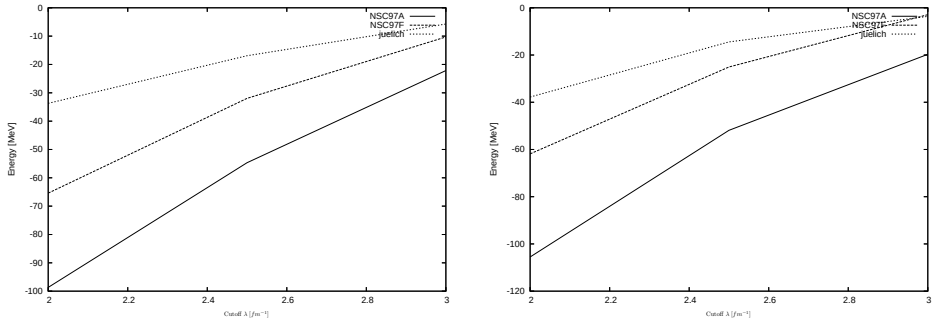

(c) $\hbar\omega = 15$ (d) $\hbar\omega = 20$

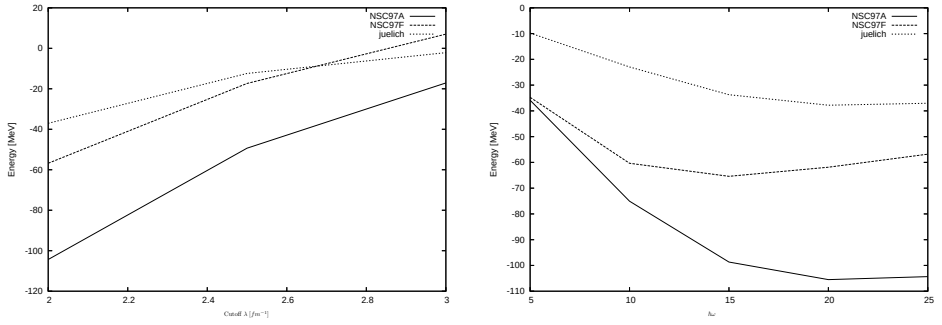

(e) $\hbar\omega = 25$ (f) $k\_cutoff = 2.0$

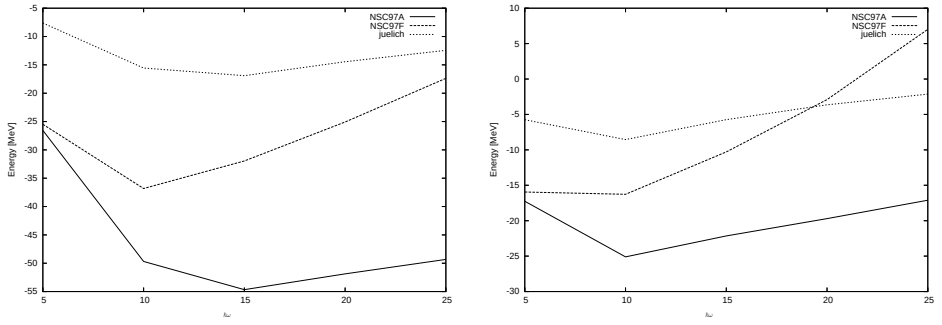

(g) $k\_cutoff = 2.5$ (h) $k\_cutoff = 3.0$

Figure 7.26: Single particle energies in $0s_{1/2}$ for ${}^{91}_{\Lambda}Zr$

$\hbar\omega$	k_cutoff	NSC97A	NSC97F	Juelich
5.0	2.0	-.358840E+02	-.347509E+02	-.977846E+01
5.0	2.5	-.265584E+02	-.254830E+02	-.761521E+01
5.0	3.0	-.172536E+02	-.159492E+02	-.573762E+01
10.0	2.0	-.750713E+02	-.603279E+02	-.229602E+02
10.0	2.5	-.496889E+02	-.368208E+02	-.155582E+02
10.0	3.0	-.251061E+02	-.162715E+02	-.854547E+01
15.0	2.0	-.986818E+02	-.654056E+02	-.337210E+02
15.0	2.5	-.546621E+02	-.319591E+02	-.169061E+02
15.0	3.0	-.221431E+02	-.102903E+02	-.572883E+01
20.0	2.0	-.105513E+03	-.618633E+02	-.378006E+02
20.0	2.5	-.518825E+02	-.250758E+02	-.144423E+02
20.0	3.0	-.197019E+02	-.289759E+01	-.363980E+01
25.0	2.0	-.104345E+03	-.568018E+02	-.370464E+02
25.0	2.5	-.493258E+02	-.173729E+02	-.124339E+02
25.0	3.0	-.171029E+02	0.701692E+01	-.213177E+01

Table 7.5: Single particle energies for Λ in the $0s_{1/2}$ orbital outside a core of ^{90}Zr

8 Notes

9 Conclusion

References

[1] Review of Particle Physics: Journal of Physics G, Nuclear and Particle Physics, Vol 33, 2006

[2] T. Nakano et al.: Physical Review Letters, Volume 91, 012002

[3] Aitchinson and Hey: Gauge theories in particle physics. Third ed. Abingdon: Taylor and Francis Group, 2003

[4] Steven Weinberg: The quantum theory of fields. Paperback ed. New York: Cambridge University Press, 2005

[5] Morten Hjorth-Jensen: Lecture notes in computational physics. Oslo, 2007

[6] H. Yukawa: Proc. Phys. Math. Soc. Jpn 17, 48, 1935

[7] R. Machleidt: Adv. Nucl. Phys. 19, 189, 1989

[8] Taketani, Nakamura, Sasaki: Proc. Theor. Phys 6, 581, 1951

[9] F. Madl, G. Shaw: Quantum Field Theory. Revised ed. Chichester: John Wiley & Sons, 1993

[10] R. Machleidt: Relativistic Dynamics and Quark-Nuclear Physics. New York: Wily, 1986

[11] P.J. Ellis and E. Osnes: Rev. of Mod. Phy. Vol 49, No 4, 1977

[12] K Heyde: Basic ideas and concepts in nuclear physics. 3. ed. Bristol: IOP Publishing Ltd, 2004

[13] J.J. Sakurai: Modern Quantum Mechanics. Rev. ed. Reading: addison-wesley Publishing Company, Inc, 1994

[14] M. Rotenberg et al: The 3-j and 6-j symbols. The Technology Press, MIT, 1959

[15] A. de Shalit and I. Talmi: Nuclear Shell Theory

[16] Bogner, Kuo and Schwenk: Phys. Rep. 386, 2003

[17] Dean, Hagen, Hjorth-Jensen and Papenbrock: Effective interactions and Coupled-Cluster Theories for Stable and Unstable Nuclei, Not yet published

[18] Mary L. Boas: Mathematical methods in the physical sciences. 3. ed., John Wiley & Sons, Inc, 2006

[19] Brown & Jackson: The nucleon-nucleon interaction. North Holland publishing company, 1976